

Virtual holonomic constraint approach for planar bipedal walking robots extended to double support

Michael Scheint, Marion Sobotka, and Martin Buss

Abstract—The concept of virtual holonomic constraints is extended to the case of double support, which is characterized by a closed kinematic chain and redundancy in the state variables. An appropriate coordinate transformation is used to present the equations of motion in the coordinates of the actual degrees of freedom of the system. Virtual constraints of proper dimension lead to reduced dynamics of dimension two. The reduced dynamics is derived in a generalized way which includes previous results for the case of a single point contact. Control of the reduced dynamics is discussed in particular for the double support case. The derived concept is illustrated for a biped robot walking gait with a double support phase and an underactuated single support phase.

I. INTRODUCTION

The control of underactuated mechanical systems for periodic motions using virtual holonomic constraints has been proposed in [1], [2]. The approach has been applied to the locomotion control of underactuated bipeds [2] and extended to full actuation [3]. Control of a biped based on virtual holonomic constraints allows to investigate orbital stability on a reduced dynamics of dimension two, thus simplifying stability analysis. Parametrization of the virtual constraints permits to optimize biped motion for energy consumption.

In previous work [4], [5], the aforementioned approach was used to investigate effects of compliance on bipedal locomotion with gaits including instantaneous double support. Results in [6] show that for a simple model with compliance double support is essential. For further research on bipedal locomotion with compliance, gaits with non-instantaneous double support are of interest which motivates the presented extension of the virtual constraint approach.

During double support, the biped in contact with ground represents a closed kinematic chain where redundancy in the configuration variables and actuator inputs may arise. For the problem of optimally controlling bipedal robots during double support, several approaches have been proposed in literature [7], [8], [9], [10]. Virtual holonomic constraints are used in [8] for single support, but during double support motion is chosen as a function of time. In [10], virtual constraints are used to construct a walking gait with single and double support for the special case of a circular foot.

In this paper, the virtual constraint approach for the control of bipedal walking robots is presented in a generalized way. It is applicable for different contact situations including both single and double support. For each contact situation,

virtual holonomic constraints are enforced by feedback control which lead to reduced dynamics. Additional control of the reduced dynamics is proposed and is followed by a discussion on orbital stability of the periodic motion based on the reduced dynamics. For a planar biped, an optimized walking gait with single and double support phase is given as a numerical example.

The paper is organized as follows: The model and the considered control problem are formulated in Section 2. Transformation of the system dynamics into a constraint-free subdynamics is performed in Section 3. In Section 4, control based on the virtual holonomic constraint approach is developed. A numerical example of a biped gait is shown in Section 5. Section 6 concludes the paper with a summary.

II. MODELING AND PROBLEM FORMULATION

The control framework to be presented in this paper is intended for planar bipedal walking robots. Walking gaits are a succession of one or several different contact situations with the environment. In this section, the system dynamics are derived for the constrained system with a set of constraints given through the considered contact situation.

A. Modeling

In the following, planar mechanical systems are considered which consist of links arranged in a tree-like structure connected by prismatic or revolute joints. The system is in contact with the environment at one or more points, each of them being the end point of one branch of the tree. This results in either an open or a closed kinematic chain. The ground is considered to be perfectly rigid. It is assumed that there are no actuators at the contact points with the environment and that contact forces can act only unilaterally.

The coordinates of the system are chosen as $\mathbf{q}_e = [x_r, y_r, \mathbf{q}_a^T, \theta]^T \in \mathcal{Q}_e \subset \mathbb{R}^n$, see Fig. 1. Here, \mathbf{q}_a are the relative coordinates of the $k = n - 3$ actuated joints, θ and x_r, y_r are the absolute orientation and position of the chain with respect to the inertial world coordinate system.

The system dynamics can be derived using the Euler-Lagrange approach [11]. If the kinetic and potential energy of the system are denoted by K and V , respectively, the dynamics of the free system, i.e. no contact with the environment, are given as:

$$\frac{d}{dt} \frac{\partial K}{\partial \dot{\mathbf{q}}_e} - \frac{\partial K}{\partial \mathbf{q}_e} + \frac{\partial V}{\partial \mathbf{q}_e} = \mathbf{B}_e \mathbf{u} \quad (1)$$

with $K = \frac{1}{2} \dot{\mathbf{q}}_e^T \mathbf{D}_e(\mathbf{q}_e) \dot{\mathbf{q}}_e$, $\mathbf{B}_e^T = [\mathbf{0}^{k \times 2} \quad \mathbf{I}^{k \times k} \quad \mathbf{0}^{k \times 1}]$.

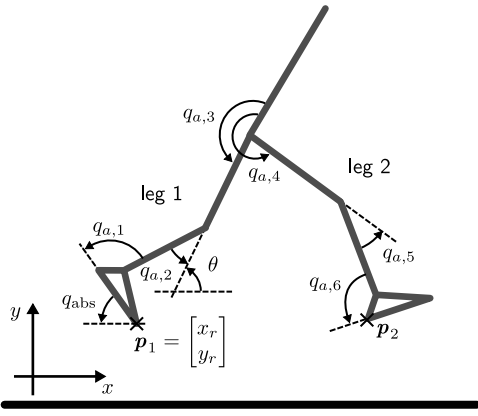


Fig. 1. Schematic picture of an exemplary biped with the chosen coordinates. The points p_1 and p_2 show possible contact points with the ground.

Here, D_e denotes the mass inertia matrix of the free system, B_e the input mapping, $\dot{q}_e = \frac{d}{dt} q_e$ are the velocities, and $u \in \mathcal{U} \subset \mathbb{R}^k$ are the actuator inputs to the system.

Definition 1 (Degree of Actuation): The system in (1) is said to be *underactuated* if the number of actuators k is less than the number of degrees of freedom. If the number of actuators is larger than the number of degrees of freedom, the system is said to be *overactuated*. The equality case is called *fully actuated*. \triangleleft

In this paper, only underactuation of degree one is considered and for simplicity is referred to as "underactuation".

B. Problem Formulation

Depending on the contact situation with the environment, the mechanical system is subject to a set of holonomic constraints $c(q_e) = 0$ describing the manifold in which the system may evolve. The constraints enter the system dynamics via the Jacobian $J_c = \frac{\partial c}{\partial q_e}$, multiplied by the Lagrange multipliers λ [12]. Then the system dynamics of one continuous phase are

$$D_e(q_e)\ddot{q}_e + C_e(q_e, \dot{q}_e)\dot{q}_e + g_e(q_e) = B_e u + J_c^T \lambda \quad (2)$$

$$c(q_e) = 0, \quad (3)$$

where $C_e \dot{q}_e$ is the vector of Coriolis and centrifugal forces and $g_e = \frac{\partial V}{\partial q_e}$ is the vector of gravitational forces. As the control concept presented here aims only at walking gaits with no flight phase, a restricting assumption is made:

Assumption 1: Only contact situations with at least one point of the kinematic chain being in contact with the environment are considered, $\dim(c) = m \geq 2$. Furthermore, the constraints are required to be independent,

$$\text{rank} \left(\frac{\partial c}{\partial q_1} \right) = m \quad \text{with } \dim(q_1) = m,$$

i.e. there exists a subset of coordinates q_1 of q_e for which the constraint Jacobian is full rank. \triangleleft

Hence, the constraints c are subdivided as $c = [c_0^T, \tilde{c}^T]^T$ where $c_0 \in \mathbb{R}^2$ specifies the position of an endpoint p_1 of the kinematic chain in world coordinates. Another restriction is posed on the point p_1 :

Assumption 2: The point p_1 is assumed to be constant w.r.t time in world coordinates:

$$c_0 = p_1(q_e) - \begin{bmatrix} x_1 \\ y_1 \end{bmatrix} = \mathbf{0} \quad \text{with} \quad \frac{d}{dt} \begin{bmatrix} x_1 \\ y_1 \end{bmatrix} = \mathbf{0}.$$

This excludes rolling contacts, e.g. by a circular foot. \triangleleft

Remark 1: As a result of Assumptions 1 and 2, the following contact situations can occur as shown in Fig. 1. For $m = 2$, an ideal point contact exists, e.g. rotation about p_1 , the toe tip of leg 1. An additional constraint ($m = 3$) can fix the foot of leg 1 to be flat on the ground or could give a sliding contact at the heel of leg 2. For $m \geq 4$, a closed kinematic chain exists as each foot has ground contact.

For a walking gait consisting of a sequence of different contact situations, the overall task is to find a set of virtual holonomic constraints which give rise to a periodic and orbitally stable walking gait. For a certain contact situation, the system dynamics in the remaining degrees of freedom are needed for designing the virtual constraints. To this end, a coordinate transformation is proposed in the next section.

III. PROJECTION OF SYSTEM DYNAMICS

The dynamic equation given in (2) is of dimension n , but the actual degrees of freedom in the system are reduced by the constraint equation to $n - m$. For position control, it is desired to find an alternative representation of the system dynamics in a reduced form without any contact force λ entering the equation. For this purpose, a proper coordinate transformation is now presented.

A. Coordinate Transformation

The coordinate transformation is intended to project the system dynamics into two subspaces, the constraint force subspace and the free velocity subspace. The latter one includes the remaining degrees of freedom of the system. In this paper, this separation is performed using the coordinate transformation developed in [13].

Proposition 1: There exists a function $\Omega : \mathcal{Q}_\Omega \rightarrow \mathbb{R}^m$ on an open set $\mathcal{Q}_\Omega \subset \mathbb{R}^{n-m}$, such that the constraint equation (3) can be rewritten as:

$$c(\Omega(q_2), q_2) = \mathbf{0} \quad \forall q_2 \in \mathcal{Q}_\Omega \quad (4)$$

$$\text{with } [q_1^T \quad q_2^T]^T = P q_e, \quad q_1 \in \mathbb{R}^m, \quad q_2 \in \mathbb{R}^{n-m}. \quad (5)$$

Here, P is an invertible matrix representing a possible necessary coordinate permutation. In the following, $P = I$ is assumed. In case of constraints with $\frac{\partial c_i}{\partial q_2} = \mathbf{0}$, the respective function Ω_i is a function of some constants. \triangleleft

Proof: The existence of Ω is given by the implicit function theorem. Suppose there exists q_{e0} such that $c(q_{e0}) = \mathbf{0}$. Assumption 1 assures that $\frac{\partial c}{\partial q_1}$ is non-singular, hence Ω exists on an open set. \blacksquare

Now define a coordinate transformation $\varphi(q_e) : \mathcal{Q}_t \rightarrow \mathcal{Q}_w$ with $\mathcal{Q}_t = \{q_e \mid c(q_e) = \mathbf{0} \wedge q_2 \in \mathcal{Q}_\Omega\} \subset \mathbb{R}^n$ and $\mathcal{Q}_w \subset \mathbb{R}^n$ from coordinates q_e to w .

$$w = \begin{bmatrix} w_1 \\ w_2 \end{bmatrix} = \varphi(q_e) = \begin{bmatrix} q_1 - \Omega(q_2) \\ q_2 \end{bmatrix} \quad (6)$$

The transformation φ is invertible and also the inverse transformation $q_e = \varphi^{-1}(w)$ is invertible on \mathcal{Q}_t . Therefore, φ is a local diffeomorphism and a valid change of coordinates. The coordinate transformation (6) is used together with

$$J_w = \frac{\partial \varphi(q_e)}{\partial q_e} \quad J_w^{-1} = \frac{\partial \varphi^{-1}}{\partial w} \quad \dot{q}_e = J_w^{-1} \dot{w} \quad (7)$$

in the next section to transform the system dynamics (2).

B. Transformed System Dynamics

After performing the change of coordinates (6), the transformed dynamic equations are partitioned in the following into the equations of motion in w_2 and contact force equations.

Lemma 2: Under the coordinate transformation in (6), the dynamics of the system are given by

$$\tilde{D}_e \ddot{w} + \tilde{C}_e \dot{w} + \tilde{g}_e = \tilde{B}_e u + \tilde{J}_c^T \lambda \quad (8)$$

with the new system matrices defined as

$$\begin{aligned} \tilde{C}_e(w, \dot{w}) &= J_w^{-T} (D_e \frac{d}{dt} J_w^{-1}) + C_e J_w^{-1} \\ \tilde{D}_e(w) &= J_w^{-T} D_e J_w^{-1} \quad \tilde{g}_e(w) = J_w^{-T} g_e \\ \tilde{B}_e(w) &= J_w^{-T} B_e \quad \tilde{J}_c^T(w) = J_w^{-T} J_c^T. \end{aligned} \quad (9)$$

Proof: Take the time derivative of \dot{q}_e in (7) and substitute it into (2). Then multiply the system of equations with J_w^{-T} . The new inertia matrix \tilde{D}_e can also be found through the independence of the kinetic energy K with respect to coordinate transformations. ■

Proposition 3: If the constraint equation (3) is fulfilled and Assumption 1 holds, then under the coordinate transformation (6) \tilde{J}_c is given as

$$\tilde{J}_c = \frac{\partial c(\varphi^{-1}(w))}{\partial w} = \begin{bmatrix} \tilde{J}_{c,1} & \mathbf{0}^{m \times n-m} \end{bmatrix} \quad (10)$$

with $\tilde{J}_{c,1} = \frac{\partial c(\Omega(w_2), w_2)}{\partial w_1}$ being invertible. ◁

Proof: The statement in (10) can be derived from Assumption 1. As $c(\Omega(q_2), q_2) = \mathbf{0} \forall q_2 \in \mathcal{Q}_\Omega$ it follows with $q_2 = w_2$ that $\frac{\partial c(\Omega(w_2), w_2)}{\partial w_2} = \mathbf{0}^{m \times n-m}, \forall w_2 \in \mathcal{Q}_\Omega$. The invertibility of $\tilde{J}_{c,1} = \frac{\partial c(q_e)}{\partial q_1} \frac{\partial q_1}{\partial w_1}$ can be concluded as the first component is invertible by Assumption 1 and the second component is an identity matrix according to the first m equations of (6). ■

Under the assumption that the constraints (3) are satisfied ($c \equiv \mathbf{0}$), the system dynamics (8) can be further simplified as $w = [\mathbf{0}^{m \times 1}, w_2^T]^T$ (similarly for \dot{w}, \ddot{w}). Now (8) can be split up, with the dynamics of w_2 being independent of λ .

$$D_\lambda \ddot{w}_2 + C_\lambda \dot{w}_2 + g_\lambda = B_\lambda u + \tilde{J}_{c,1}^T \lambda \quad (11)$$

$$D_w \ddot{w}_2 + C_w \dot{w}_2 + g_w = B_w u \quad (12)$$

Here, the matrices $D_\lambda, D_w, C_\lambda, C_w$ are obtained as proper submatrices of \tilde{D}_e, \tilde{C}_e , respectively. The components \tilde{g}_e, \tilde{B}_e are split in m and $n-m$ rows to find $g_\lambda, g_w, B_\lambda, B_w$. A definition which is needed in later derivation is now stated:

Definition 2: A variable $w_{2,i}$ from the coordinates w_2 is said to be *cyclic* with respect to (12), if $\frac{\partial D_w}{\partial w_{2,i}} \equiv \mathbf{0}$. ◁

For the chosen coordinates in Fig. 1, variable θ is cyclic in single support. The new input matrix B_w can be further subdivided, with u_1 and u_2 being the actuation of q_1 and q_2 , respectively.

$$B_w u = B_{w,1} u_1 + B_{w,2} u_2 \quad (13)$$

$$B_{w,1} = \left(\frac{\partial \tilde{\Omega}}{\partial w_2} \right)^T, \quad B_{w,2} = \begin{bmatrix} \mathbf{I}^{n-m-1} \\ \mathbf{0}^{1 \times (n-m-1)} \end{bmatrix}, \quad u = \begin{bmatrix} u_1 \\ u_2 \end{bmatrix}$$

As in B_e the first two rows are zero, only $\tilde{\Omega}$ appears, i.e. rows three to m of Ω . Rewriting (12) in state-space form with $x = [w_2^T, \dot{w}_2^T]^T$ and $G \in \mathbb{R}^{(n-m-1) \times (n-3)}$ gives

$$\dot{x} = f(x) + G(x)u. \quad (14)$$

which is used in the next section to develop control for the virtual holonomic constraints.

IV. CONTROL

The concept of virtual holonomic constraints has been successfully used for the control of underactuated systems [1], [14]. Enforcing the virtual constraints by control creates a reduced system dynamics, called zero dynamics. Here, $n-m-1$ virtual holonomic constraints are chosen for which reduced dynamics, control and stability are discussed.

A. Virtual Holonomic Constraints

For the purpose of designing virtual holonomic constraints, the coordinate vector w_2 of the system in (12) is split up into $w_2 = [w_a^T, \theta]^T$ with w_a being the vector of the remaining actuated joint coordinates. The desired evolution h_d of coordinates w_a is chosen to be a function of θ , thus the dimension of the output function is $n-m-1$.

$$y = w_a - h_d(\theta) = h(w_2). \quad (15)$$

Assumption 3: There is at least one point $w_{2,0} \in \mathcal{Q}_\Omega$ such that $h(w_{2,0})$ vanishes. Furthermore, the function $[h(w_2)\theta]^T : \mathcal{Q}_\Omega \rightarrow \mathbb{R}^{n-m}$ is a diffeomorphism. ◁

Using input/output linearizing state feedback and an appropriate controller, the output functions (15) are driven to zero, i.e. $h = \mathbf{0}$ and the Lie-derivative $\mathcal{L}_f h = \mathbf{0}$. The remaining dynamics is of dimension one and order two, and its state variables are the angle θ and $\sigma = \frac{\partial}{\partial \theta} K$, the momentum conjugate to θ . In the next section, attention is now turned to the dynamics in θ and σ .

B. Zero Dynamics

The number of outputs chosen in (15) is exactly one less than the dimension of the configuration w_2 of the reduced system dynamics (12). If the outputs in (15) are driven to zero by feedback control, then the remaining dynamics in θ, σ are called zero dynamics. Assuming $y \equiv \mathbf{0}$, the system is restricted to the submanifold \mathcal{Z} of \mathcal{X} [14].

$$\mathcal{Z} = \{x \in \mathcal{X} \mid h(x) = \mathbf{0}, \mathcal{L}_f h(x) = \mathbf{0}\} \quad (16)$$

On \mathcal{Z} , $w_2^T = [h_d(\theta)^T \theta]$, and $\dot{w}_2^T = [(\frac{\partial h_d}{\partial \theta})^T \mathbf{1}] \dot{\theta}$ holds, and the time derivative of θ is given as

$$\dot{\theta} = \frac{1}{I(\theta)} \sigma \quad \text{with} \quad I(\theta) = D_{w,n-m} \begin{bmatrix} \frac{\partial h_d}{\partial \theta} \\ \mathbf{1} \end{bmatrix} \quad (17)$$

where $D_{w,n-m}$ is the $(n-m)$ -th (i.e. last) row of D_w . The time derivative of σ in turn is in general

$$\begin{aligned} \frac{d}{dt}\sigma = & -C_{w,n-m}\dot{w}_2 - g_{w,n-m} + \mathbf{b}^T \mathbf{u}_1 \\ & + \dot{w}_2^T \left(\frac{\partial}{\partial w_2} D_{w,n-m} \right)^T \dot{w}_2 \end{aligned} \quad (18)$$

with $\mathbf{b} = \frac{\partial \tilde{\Omega}}{\partial \theta} \in \mathbb{R}^{m-2}$. Hence, the zero dynamics can be summarized as a set of differential equations in θ, σ :

$$\begin{aligned} \dot{\theta} &= \kappa_1(\theta)\sigma = \frac{1}{I(\theta)}\sigma \\ \dot{\sigma} &= \kappa_2(\theta, \sigma) + \kappa_3(\theta) + \mathbf{b}^T \mathbf{u}_1. \end{aligned} \quad (19)$$

This is the general representation of the zero dynamics for $m \geq 2$ created by the virtual constraints in (15). Previous results for a point contact are a special case of (19) as shown in the following remark.

Remark 2: For an open kinematic chain, i.e. either point contact with $m = 2$ or flat foot contact $m = 3$, θ is a cyclic variable. Then, (19) results in ($b = 0$ for $m = 2$):

$$\dot{\sigma} = \kappa_3(\theta) + b u_1 = -g_{w,n-m}(\theta) + b u_1. \quad \triangleleft$$

Proposition 4: For $m \geq 3$, the vector \mathbf{b} in (19) is nonzero, i.e. $\mathbf{b} \neq \mathbf{0}$. Moreover, for double support it holds that $\mathbf{b} = \mathbf{b}(\theta)$ with $\frac{\partial \mathbf{b}}{\partial \theta} \neq \mathbf{0}$.

Proof: The proof is shown in appendix A. \blacksquare

Proposition 5: In case of a closed kinematic chain, i.e. both feet in contact with the ground, the variable θ is not a cyclic variable. \triangleleft

Proof: The proof is shown in appendix B. \blacksquare

The consequences of Proposition 4 and 5 are that neither $\mathbf{b}^T \mathbf{u}_1$ nor $\kappa_2(\theta, \sigma)$ vanish in general from (19). Hence, $\dot{\sigma}$ is indeed a function of θ, σ and controllable by \mathbf{u}_1 .

The set of equations (19) governs the complete dynamics as the output functions in (15) are a function of θ . If the system is restricted to the manifold \mathcal{Z} , stability analysis of (19) is valid for the complete dynamics. Based on the zero dynamics, control is discussed in the next subsection.

C. Control

In this subsection control is developed first for the zero dynamics and second for enforcing the virtual holonomic constraints. Control input appears in the zero dynamics (19) only for $m > 2$. For $m = 2$, i.e. underactuation of degree one, the zero dynamics are autonomous and are completely determined by the choice of \mathbf{h}_d . Therefore, the control of the zero dynamics developed here is only applicable to cases with $m > 2$ while the feedback control for the outputs \mathbf{y} hold for all cases $m \geq 2$.

For the control of the zero dynamics a virtual holonomic constraint for σ is proposed, i.e. σ shall follow a desired evolution as a function of θ .

$$y_\sigma = \sigma - h_{d,\sigma}(\theta) \quad (20)$$

Using the second equation of (19), the feedback linearizing control is given as

$$\mathbf{u}_1 = \mathbf{b}^+ \left(v_\sigma - \kappa_2 - \kappa_3 + \frac{\partial h_{d,\sigma}}{\partial \theta} \frac{h_{d,\sigma}(\theta)}{I(\theta)} \right) \quad (21)$$

where v_σ is the control input to the linearized system and \mathbf{b}^+ is the pseudo-inverse of \mathbf{b} . This solution to \mathbf{u}_1 minimizes the components of \mathbf{u}_1 . A possible choice for the control law for v_σ is $v_\sigma = -k_p y_\sigma$, with k_p being some positive constant. Due to modeling requirements, a dynamic saturation for \mathbf{u}_1 can be necessary [3].

Proposition 6: The vector \mathbf{b}^+ is non-zero $\forall \theta$.

Proof: Proposition 4 ensures that $\mathbf{b} = \frac{\partial}{\partial \theta} \tilde{\Omega} \neq \mathbf{0}$. Hence, the product $\mathbf{b}^T \mathbf{b}$ is strictly positive. As \mathbf{b}^+ is given as $\mathbf{b}^+ = \mathbf{b}(\mathbf{b}^T \mathbf{b})^{-1}$, \mathbf{b}^+ must be non-zero. \blacksquare

For the feedback linearizing control of the virtual constraints (15) the remaining input vector \mathbf{u}_2 is used. Twice time-differentiation of (15) gives:

$$\ddot{\mathbf{y}} = \mathbf{H}_d \ddot{w}_2 - \frac{\partial^2 \mathbf{h}_d}{\partial \theta^2} \dot{\theta}^2, \quad \mathbf{H}_d = \left[\mathbf{I}^{n-m-1} - \frac{\partial \mathbf{h}_d}{\partial \theta} \right]. \quad (22)$$

Using (12), (13) the control law for \mathbf{u}_2 is found as

$$\mathbf{u}_2 = (\mathcal{L}_G \mathcal{L}_f \mathbf{h})^{-1} (v - \mathcal{L}_f^2 \mathbf{h}) \quad (23)$$

$$\text{with} \quad \mathcal{L}_G \mathcal{L}_f \mathbf{h} = \mathbf{H}_d \mathbf{D}_w^{-1} \mathbf{B}_{w2} \quad (24)$$

$$\mathcal{L}_f^2 \mathbf{h} = \mathbf{H}_d \mathbf{D}_w^{-1} (\mathbf{B}_{w1} \mathbf{u}_1 - \mathbf{C}_w \dot{w}_2 - \mathbf{g}_w) - \frac{\partial^2 \mathbf{h}_d}{\partial \theta^2} \dot{\theta}^2 \quad (25)$$

where v denotes the control input to the linearized system. In order to assure $\mathbf{y} \equiv \mathbf{0}$ a finite-time stabilizing controller can be used for v . The validity of the feedback linearizing control is given by the following assumption.

Assumption 4: The set of output functions in (15) is chosen such that $\mathcal{L}_G \mathcal{L}_f \mathbf{h}(w_2)$ and $I(\theta)$ defined in (24) and (17) are both invertible on the open set \mathcal{Q}_Ω .

For the system under feedback control (21), (23), orbital stability is discussed next based on the zero dynamics.

D. Orbital Stability

For biped walking, the stability of a periodic orbit can be analyzed using the Poincaré return map. Evaluating this criterion on the full system is computational expensive. Theorem 4.5 in [14] states requirements under which the orbital stability can be deduced from the restricted Poincaré map of the reduced system dynamics (19). Main requirements are that the manifold \mathcal{Z} (16) is an embedded submanifold of \mathcal{X} , \mathcal{Z} is locally continuously finite-time attractive, and \mathcal{Z} is (hybrid) invariant.

It is assumed that the requirements are met using an appropriate controller for v . Then the Poincaré section \mathcal{P} restricted to the zero dynamics can be chosen as:

$$\mathcal{P} \cap \mathcal{Z} = \{(\theta, \sigma) \mid \theta = \theta^-\} \quad (26)$$

where θ^- is a certain point of the periodic motion, e.g. just before impact. As a result, evaluating the Poincaré map for the zero dynamics reduces to evaluate $\sigma(\theta^-)$ for successive cycles to obtain the eigenvalue μ of the discrete map $\sigma_{k+1}(\theta^-) = \mu \sigma_k(\theta^-)$. For $m = 2$, results can be found in [2]. For the case of $m > 2$, i.e. when $\dim(\mathbf{b}) \geq 1$, stability of the periodic motion mostly depends on the convergence properties of the controller for $h_{d,\sigma}$. Control input v_σ is however bounded as restrictions on contact force may not be violated.

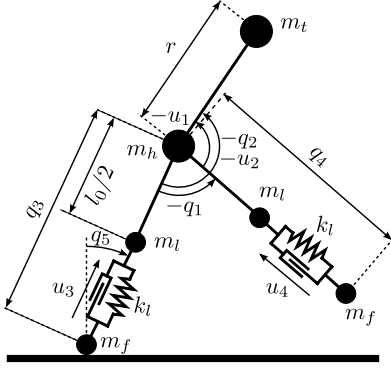


Fig. 2. Planar biped model with point masses shown. Angles and torques are measured positive in clockwise direction.

V. SIMULATION

In this section, the presented method is applied to the control of the planar biped shown in Fig. 2. The biped has point feet, two legs each with a prismatic joint, two revolute joints at the hip and a torso. At the leg joints, linear springs work in parallel to the actuators. More details on the biped model can be found in [4]. The goal is a periodic and orbital stable gait consisting of two phases, single support and double support. In single support, the biped is underactuated as the angle q_5 is not actuated. In double support, the biped is overactuated with three degrees of freedom.

In the following, variables from single support are denoted by an additional subscript s while the variables from double support are denoted by an additional subscript d .

A. Hybrid Model

The considered biped gait can be modeled as a hybrid system, consisting of two continuous phases separated by instantaneous transitions occurring at foot touchdown and foot liftoff. Transitions take place if the state enters the corresponding switching set, \mathcal{S}_s^d for impact and \mathcal{S}_d^s for liftoff.

$$\mathcal{S}_s^d = \{\mathbf{x}_s \mid p_2^y(\mathbf{x}_d) = 0\}, \quad \mathcal{S}_d^s = \{\mathbf{x}_d \mid \theta = \theta_d^-\} \quad (27)$$

Here, the angle θ_d^- denotes the angle θ at liftoff and represents a gait parameter. Impact is modeled as perfectly inelastic with impulsive collision forces and no slip or rebound is supposed to occur. The impact equation can be derived from the momentum balance using (1) [8], which is not altered by the springs as they are in parallel to joints. After computing the state after impact, a coordinate relabelling is applied to change the reference leg. The transition from single support to double support is expressed as:

$$\mathbf{x}_d^+ = \Delta_s^d(\mathbf{x}_s^-). \quad (28)$$

No collisions are included at transition from double support to single support, positions and velocities are continuous:

$$\mathbf{x}_s^+ = \Delta_d^s(\mathbf{x}_d^-) = \mathbf{x}_d^-. \quad (29)$$

The transitions together with the dynamics (2) constitute the hybrid model, illustrated in Fig. 3.

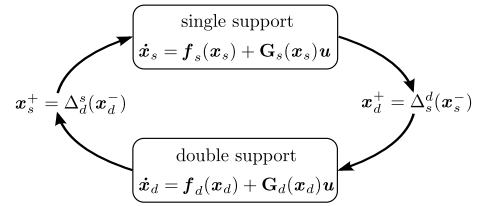


Fig. 3. The hybrid model of the walking gait with two continuous phases, single support and double support. Transitions occur at swing foot impact and swing foot lift off.

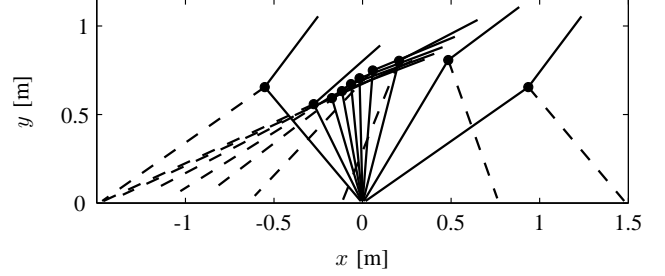


Fig. 4. Stick-figure plot of the optimized biped gait. Biped posture is shown at 10 equally distributed time instances starting with double support. Stance foot and torso are shown solid, swing foot shown dashed.

B. Parametrization

The biped gait is determined by the choice of \mathbf{h}_d in the virtual holonomic constraints (15) for both phases and by the choice of $\mathbf{h}_{d,\sigma}$ (20). The virtual constraints are required to be transition invariant, i.e. if the virtual constraints are fulfilled ($\mathbf{y}(\mathbf{x}) = \mathbf{0}$) in phase i , then the state after transition should also fulfill the constraints. The functions \mathbf{h}_d are chosen here as Beziér polynomials with the free polynomial coefficients \mathbf{a}_s , \mathbf{a}_d , \mathbf{a}_σ being the optimization parameters. Other free parameters are the spring constant k_s and the aforementioned angle θ_d^- for foot liftoff. The free parameters are summarized in $\gamma = [\mathbf{a}_s^T, \mathbf{a}_d^T, \mathbf{a}_\sigma^T, k_s, \theta_d^-]$.

C. Optimization

Optimization is used to determine a set of parameters γ which do not violate modeling requirements and which minimize the integral over squared inputs.

$$\begin{aligned} \min_{\gamma} \quad & \frac{1}{L_s(\gamma)} \int_0^{T_s(\gamma)} \|\mathbf{u}^*(t, \gamma)\|_2^2 dt \quad (30) \\ \text{s.t.} \quad & \mathbf{n}_{iq}(\gamma) \leq \mathbf{0} \\ \text{with} \quad & \mathbf{u}^* = \mathbf{u}|_{v=0} - k_s [\mathbf{0}^{2 \times 1} \quad q_3 \quad q_4] \end{aligned}$$

Here, L_s denotes step length, T_s denotes step time, \mathbf{n}_{iq} are the nonlinear constraints and \mathbf{u}^* is the reference actuator input for staying on the zero dynamics. The nonlinear constraints include the average walking speed is required to be within a certain range δv of the desired speed. Furthermore, the contact forces λ must be unilateral and within the friction cone. The same applies for the impulsive forces at impact. Another constraint specifies the angle θ to be monotonically increasing between impacts, i.e. $\dot{\theta} > 0$.

The SQP based solver *fmincon* under Matlab was used for optimization. Desired speed v_{des} was set to $0.9 \frac{\text{m}}{\text{s}}$ with a tolerance of $\pm 0.01 \frac{\text{m}}{\text{s}}$. The friction coefficient was set to 0.7.

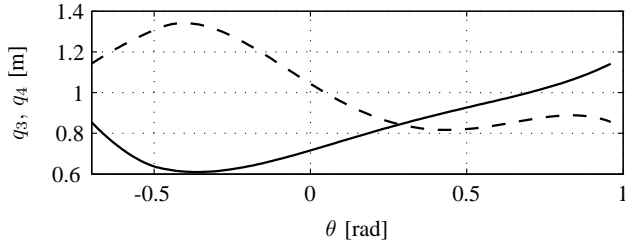


Fig. 5. Variables q_3, q_4 over θ for the optimized gait. Stance leg length q_3 depicted with solid line, swing leg length q_4 depicted with dashed line. Start of plot is at impact.

D. Result

Optimized costs are $3.9 \cdot 10^4 \text{ N}^2 \text{ ms}$ with a spring stiffness of $k_s = 742 \frac{\text{N}}{\text{m}}$. The duration of double support being a function of the parameters γ is 8% of total step time which is rather short.

The optimized walking gait is shown for one step in Fig. 4 using a stick-figure plot. The step starts just after impact, followed by double support and then single support. During swing, the swing foot is above the ground. Although forward leaning of the torso and step length are rather large, the sinusoidal motion of the hip seems quite natural. The evolution of the leg lengths q_3, q_4 over θ is shown in detail in Fig. 5. During double support, q_3, q_4 are not part of the coordinate vector w_2 .

VI. CONCLUSIONS

The virtual constraint approach was extended in this paper for the control of bipedal robots in double support. In double support, redundancy in the configuration variables exists and the equations of motion for the remaining degrees of freedom were derived. Virtual holonomic constraints were used to create a zero dynamics of order two, for which control and stability was discussed. A numerical example of a planar bipedal gait with single support and double support was shown. Future work will concentrate on considering the contact force restrictions in the control of the zero dynamics.

ACKNOWLEDGMENTS

This work was supported in part within the Grant WO1440/2-1 of the German Research Foundation (DFG).

APPENDIX

A. Proof of Proposition 4

For $m \geq 3$ two possibilities exist for the constraints. Either a point and the absolute angle is fixed ($m = 3$), i.e. one foot flat on the ground. Or on each foot one point is constrained ($m \geq 3$). In the first case, the constraint on the angle q_{abs} (Fig. 1) can be written as $q_{\text{abs}} - c_a^T q_a - c_\theta \theta = \text{const.}$ with c_θ necessarily non-zero as the absolute orientation of the biped is required to express q_{abs} . Hence, $\frac{\partial \tilde{\Omega}}{\partial \theta} = c_\theta \neq 0$.

For the second case, one component of \tilde{c} contains a position coordinate of a point on the second foot. The transformation from a point p_1 on foot one to a point p_2 on foot two is given by a homogeneous transformation [11]

$$\begin{bmatrix} p_2 \\ 1 \end{bmatrix} = H \begin{bmatrix} p_1 \\ 1 \end{bmatrix} \text{ with } H = H_0(q_{\text{abs}})H_1(q_{a,1}) \dots H_k(q_{a,k}).$$

As q_{abs} is an angle, H_0 includes a rotation matrix which is nonlinear in q_{abs} . Hence, if $c = [p_1^T \ p_{2,i} \ \dots]^T$, then $\tilde{\Omega}$ is nonlinear function of q_{abs} . The angle q_{abs} in turn is as above a function of θ . Therefore, it can be concluded that $\frac{\partial \tilde{\Omega}}{\partial \theta} = \epsilon(\theta)$ with $\frac{\partial \epsilon}{\partial \theta} \neq 0$, which together with the definition $b = \frac{\partial \tilde{\Omega}}{\partial \theta}$ closes the proof. ■

B. Proof of Proposition 5

From (9) and (8), the matrix D_w is given as

$$D_w = \left(\frac{\partial \Omega}{\partial w_2} \right)^T \left(D_{11} \frac{\partial \Omega}{\partial w_2} + D_{12} \right) + D_{21} \frac{\partial \Omega}{\partial w_2} + D_{22}$$

with $D_e = \begin{bmatrix} D_{11} & D_{12} \\ D_{21} & D_{22} \end{bmatrix}$.

Matrix D_{11} is a positive definite matrix as D_e is positive definite. The proof of Proposition 4 shows that $\frac{\partial^2 \tilde{\Omega}}{\partial \theta^2} \neq 0$. Therefore, $\left(\frac{\partial \Omega}{\partial w_2} \right)^T D_{11} \frac{\partial \Omega}{\partial w_2}$ is a function of θ and hence $D_w = D_w(\theta)$. Thus under definition 2, θ is not cyclic. ■

REFERENCES

- [1] A. Shiriaev, J. Perram, and C. Canudas-de Wit, "Constructive tool for orbital stabilization of underactuated nonlinear systems: Virtual constraints approach," *IEEE Trans. Automat. Contr.*, vol. 50, no. 8, pp. 1164–1176, 2005.
- [2] E. Westervelt, J. Grizzle, and D. Koditschek, "Hybrid zero dynamics of planar biped walkers," *IEEE Trans. Automat. Contr.*, vol. 48, no. 1, pp. 42–56, 2003.
- [3] J. H. Choi and J. Grizzle, "Planar bipedal walking with foot rotation," in *Proceedings of the American Control Conference (ACC)*, vol. 7, 2005, pp. 4909–4916.
- [4] M. Scheint, M. Sobotka, and M. Buss, "Compliance in gait synthesis: Effects on energy and gait," in *Proceedings of the IEEE International Conference on Humanoid Robots, Daejeon, Korea, 2008*, pp. 259–264.
- [5] T. Schaub, M. Scheint, M. Sobotka, and M. Buss, "Effects of compliant ankles on bipedal locomotion," in *Proceedings of the IEEE International Conference on Robotics and Automation (ICRA)*, Kobe, Japan, 2009, pp. 2761 – 2766.
- [6] H. Geyer, A. Seyfarth, and R. Blickhan, "Compliant leg behaviour explains basic dynamics of walking and running," *Proc R. Soc. B*, vol. 273, no. 1603, pp. 2861–2867, 2006.
- [7] G. Bessonnet, P. Seguin, and P. Sardain, "A Parametric Optimization Approach to Walking Pattern Synthesis," *The International Journal of Robotics Research*, vol. 24, no. 7, pp. 523–536, 2005.
- [8] S. Miossec and Y. Aoustin, "A Simplified Stability Study for a Biped Walk with Underactuated and Overactuated Phases," *The International Journal of Robotics Research*, vol. 24, no. 7, pp. 537–551, 2005.
- [9] D. Tlalolini, C. Chevallereau, and Y. Aoustin, "Comparison of different gaits with rotation of the feet for a planar biped," *Robotics and Autonomous Systems*, vol. 57, no. 4, pp. 371–383, 2009.
- [10] S. Srinivasan, I. A. Raptis, and E. R. Westervelt, "Low-dimensional sagittal plane model of normal human walking," *Journal of Biomechanical Engineering*, vol. 130, no. 5, p. 051017, 2008.
- [11] M. W. Spong and M. Vidyasagar, *Robot Dynamics and Control*. New York, NY, USA: John Wiley & Sons, Inc., 1989.
- [12] R. M. Murray, S. S. Sastry, and L. Zexiang, *A Mathematical Introduction to Robotic Manipulation*. Boca Raton, FL, USA: CRC Press, Inc., 1994.
- [13] N. McClamroch and D. Wang, "Feedback stabilization and tracking of constrained robots," *IEEE Trans. Automat. Contr.*, vol. 33, no. 5, pp. 419–426, 1988.
- [14] E. Westervelt, J. Grizzle, C. Chevallereau, J. Choi, and B. Morris, *Feedback control of dynamic bipedal robot locomotion*. Boca Raton: CRC Press, 2007.